Inversion of real and complex phase shifts to potentials by the generalized Cox-Thompson inverse scattering method at fixed energy

O. Melchert[1], W. Scheid[1], and B. Apagyi[2]

[1]Institut für Theoretische Physik der Justus-Liebig-Universität,
D-35392 Giessen, Germany

[2]Department of Theoretical Physics, Budapest University of
Technology and Economics, H-1111 Budapest, Hungary

March 14, 2006

Abstract

Cox-Thompson inverse scattering method at fixed energy has been generalized to treat complex phase shifts derived from experiments. New formulas for relating phase shifts to shifted angular momenta are derived. The method is applied to phase shifts of known potentials in order to test its quality and stability and further, it is used to invert experimental n-α and n-^{12}C phase shifts.

1. Introduction

Since its discovery in the fifties of the last century, inverse quantum scattering theory [1] attracts a constant interest. For the case of inverse scattering at fixed energy, there exist different schemes giving rise to potentials of different families. For example, the rational expansion of the S-matrix (due to Jost) results in an analytical form of inverse potentials, studied in detail by Lipperheide and Fiedeldey [2]. An alternative formulation of fixed energy inverse quantum scattering theory has been developed by Newton and Sabatier [3] (NS) and this theory was modified and applied to practical problems by Münchow and Scheid [4] (mNS). The NS inversion theory leads to a potential family with zero first momentum ($\int_0^\infty U(r) \ r \ dr = 0$) if a finite set of phase shifts is used. This is an obvious severe restriction on the sphere of validity of the resulting inversion potentials. Moreover, the NS inversion potential also possesses an unavoidable singularity of the type α/r near the origin, with α being a free parameter characterizing the infinity of phase equivalent inversion potentials of the NS scheme. A more recent review about the quantum mechanical inversion problem and its application to nuclear scattering has been given by Kukulin and Mackintosh [5] where further references related with this problem can be found.

In this paper we investigate and develop further a particular nonlinear type of inverse quantum scattering procedure at fixed energy. This theory has been originally proposed by Cox and Thompson [6] (CT) and applied recently in Ref. [7] to invert finite sets of *real* phase shifts generated from known model potentials. The CT inversion scheme yields an inversion potential which has a finite first momentum and may possess a finite value at the origin [6,7].

We shall extend the CT method to the inversion of *complex* phase shifts. In particular, we shall demonstrate the quality of the inversion method on examples

with given potentials and on data from neutron(n)-nucleus scattering. In order to use complex phase shifts we continue the non-physical (shifted) angular momenta $\{L\}$ of the CT method to the complex plane from the real values $(-\frac{1}{2}, \infty)$ as originally proposed by Cox and Thompson [6]. We also present a simpler version of the non-linear equations than that given in Ref. [7], which has to be solved for complex angular momenta $\{L\}$ with complex input phase shifts $\{\delta\}$. For the solution we apply various non-linear solvers, both direct (as e.g. Newton-Raphson) and stochastic (as e.g. simulated annealing) ones.

In section 2 a short formulation of the CT method generalized to complex phase shifts is outlined. In section 3 we compare the CT method with the modified NS method by using complex phase shifts of given potentials and apply the CT method by inverting elastic phase shifts of the n-α and n-^{12}C scattering derived from experimental differential cross sections. Section 4 concludes about the necessity of a further development of the CT method to enable its application to Coulomb systems. Some calculational details are given in the Appendix.

2. Theory

The new step in this paper is that we consider the inversion of complex phase shifts to a complex potential by using the CT method which has been up to now developed for real phases only. We define the CT inverse potential, which is assumed to be complex-valued, as

$$V(r) = -\frac{2}{r}\frac{d}{dr}\frac{K(r,r)}{r} = -\frac{2}{r^2}\left(\frac{dK(r,r)}{dr} - \frac{K(r,r)}{r}\right) \tag{1}$$

3

with the diagonal transformation kernel [6]

$$K(r,r) = \sum_{L \in T} A_L(r) u_L(r). \tag{2}$$

Now we have to introduce complex indices $L \in T$ which are taken from a set T of generalized (shifted) angular momentum quantum numbers being disjunct with the set $\{l\} \equiv S$ of real integer physical angular momenta: $T \bigcap S = \{\}$.

In Eq. (2), the function $u_L(r)$ denotes the regular Riccati-Bessel function which satisfies the free Schrödinger equation

$$-u_L''(r) + \frac{L(L+1)}{r^2} u_L(r) = k^2 u_L(r) \tag{3}$$

with the behavior $u_L \sim r^{L+1}$ at the origin, and k is the wave number corresponding to the fixed energy $E = \hbar^2 k^2 / 2\mu$, where μ is the reduced mass of the scattering system. It is obvious that u_L depends only on the dimensionless quantity $x = kr$, and we can choose throughout $k = 1$. For the case $k \neq 1$ we get the potentials as $U(r) = E \cdot V(x)$.

All information on the potential is encoded into the functions $A_L(r)$ of Eq. (2), and the generalized angular momentum quantum numbers $\{L\}$. The functions $A_L(r)$ can be determined by starting with the Gel'fand-Levitan-Marchenko–type integral equation for the transformation kernel

$$K(r,\rho) = g(r,\rho) - \int_0^r ds \, s^{-2} \, K(r,s) g(s,\rho), \quad r > \rho \tag{4}$$

and then applying the CT ansatz [6] for the symmetric kernel

$$g(r,\rho) = \sum_{l \in S} \gamma_l u_l(r_<) v_l(r_>) = g(\rho,r), \quad r_{\{\substack{< \\ >}\}} = \left\{\begin{matrix} \min \\ \max \end{matrix}\right\} (r,\rho), \tag{5}$$

where v_l is the irregular Neumann function which satisfies Eq. (3) with the behavior r^{-l} at the origin and γ_l denotes expansion coefficients to be determined. Inserting

expansions (2) and (5) into Eq. (4) one obtains a system of linear equations for the functions $A_L(r)$ as

$$\sum_{L \in T} A_L(r) W[u_L(r), v_l(r)] / [l(l+1) - L(L+1)] = v_l(r), \quad l \in S \tag{6}$$

where the set T is, as yet, unknown. In equation (6) the usual notation for the Wronskian $W[a, b] = ab' - a'b$ has been adopted.

In Ref. [7] two systems of nonlinear equations have been set up which contain the real scattering phase shifts $\{\delta_l\}$ as input quantities and yield, upon solution, the set T of real shifted angular momenta. The derivation of the main equation which determines the complex L-values from the complex $\{\delta_l\}$ input quantities proceeds quite similarly as given in Ref. [7]. The final result can be written in the remarkably simple form

$$S_l = \frac{1 + i\mathcal{K}_l^+}{1 - i\mathcal{K}_l^-}, \quad l \in S \tag{7}$$

with the (non unitary) scattering matrix elements $S_l = \exp(2i\delta_l)$ as input, and the "shifted" reactance matrix elements which are defined as

$$\mathcal{K}_l^{\pm} = \sum_{L \in T, l' \in S} N_{lL} \left(M^{-1}\right)_{Ll'} e^{\pm i(l-l')\pi/2}, \quad l \in S \tag{8}$$

where the square matrices

$$\left\{ \begin{matrix} N \\ M \end{matrix} \right\}_{lL} = \frac{1}{L(L+1) - l(l+1)} \left\{ \begin{matrix} \sin\left((l-L)\pi/2\right) \\ \cos\left((l-L)\pi/2\right) \end{matrix} \right\}, \quad l \in S, L \in T, S \bigcap T = \{\} \tag{9}$$

contain, in a highly nonlinear way, the unknown complex L-values.

The system of nonlinear equations (7) can be cast into an equivalent form

$$\tan \delta_l = \frac{\mathcal{K}_l^+ + \mathcal{K}_l^-}{2 + i(\mathcal{K}_l^+ - \mathcal{K}_l^-)}, \quad l \in S \tag{10}$$

which proves useful during the solution processes.

5

Once the L-values are found by solving Eqs. (7) or (10) the expansion coefficients γ_l can be calculated from the expression

$$\gamma_l = \frac{\prod_{L \in T}[l(l+1) - L(L+1)]}{\prod_{l' \in S, l' \neq l}[l(l+1) - l'(l'+1)]}, \quad l \in S.$$ (11)

The search for complex L-values resulting from complex phase shifts is mathematically more complex than that for real L-values and needs advanced numerical methods like the Newton-Raphson or simulated annealing methods.

3. Results

First, we discuss the quality and stability of the CT inversion method with given complex potentials. For real short-ranged potentials these studies were partly carried out in Ref. [7]. Then in order to show the applicability of the CT method for experimental phases, we consider n-α inversion potentials at energies where the experimental phase shifts are real, and n-^{12}C inversion potentials at energies above the threshold where the experimental phase shifts are complex.

3.1 Inversion of synthetic complex phase shifts

The application of inversion methods has two sources of errors, namely the quality of the phase shift analysis of the measured differential cross section and the quality of the inversion method from the phase shifts to the potential. Here, we will concentrate our discussion on the second source of errors. As shown by Airapetyan et al. [8] and Ramm and Gutman [9], an inversion is very sensitive to very small changes in the phase shifts of piece-wise constant potentials. However, the Newton-Sabatier- and the Cox-Thompson-methods have these only to a minor extend if the searched potentials are expanded in terms of Bessel functions with smooth coefficients $A_L(r)$ (see equations (1) and (2)). The resulting potentials have oscillations around the true potential with a wave length of the order of $2\pi/k = h/\sqrt{2\mu E}$. This effect can be most clearly recognized when we invert phase shifts of given complex box potentials as demonstrated for the CT- and mNS-methods in Fig. 1. Here one recognizes the advantage of the CT-method: The inversion leads to a finite value of the potential at the origin. For a Woods-Saxon potential the inverted potentials are smoother as shown in Fig. 2.

The amplitude of the oscillations depends on the maximum angular momentum $l_{\max}$

and on the precision of the phase shifts and of the calculation. For a fixed precision of the calculation (double precision in the FORTRAN programme) we find a maximal $l_{\max}$ above which the inverted potential does not change anymore since the additional coupled equations fall below the precision of our calculation. In the case of higher incident energies the phase shifts drop slower down with angular momentum and, therefore, the inversion procedure has a higher quantity of information about the searched potential at a given precision of the programme and leads to a higher quality of the inverted potential. It is very difficult to formulate this numerical experience, which we found with our calculations, in an analytical form since the NS-and CT-equations are nonlinear. Such mathematical investigations on the stability and precision of the CT method are needed for a future advance of this ill-conditioned inversion problem.
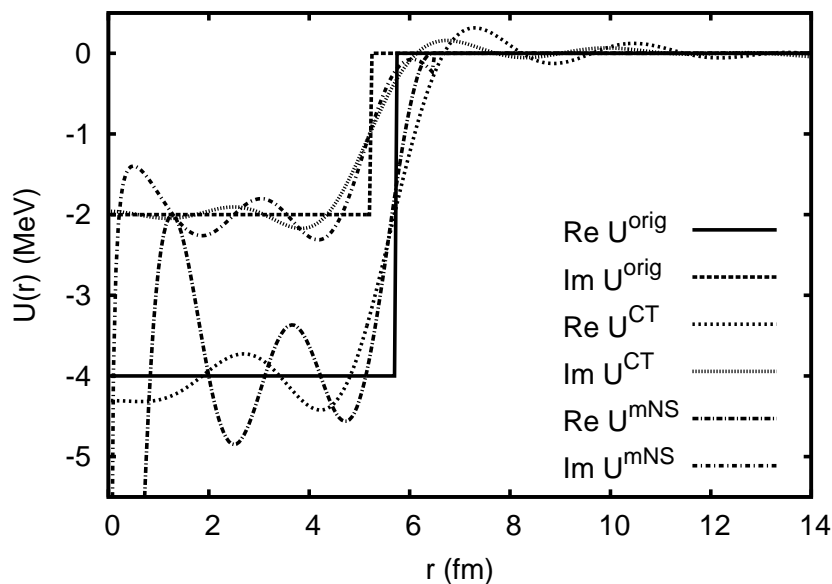

Fig. 1. Complex box potential: Results for the inversion of 11 phase shifts at $E_{cm} = 22$ MeV using the CT- and mNS-method. The masses of the scattered particles were chosen as $M_1 = M$ and $M_2 = 20 \cdot M$, where M is the nucleon mass.
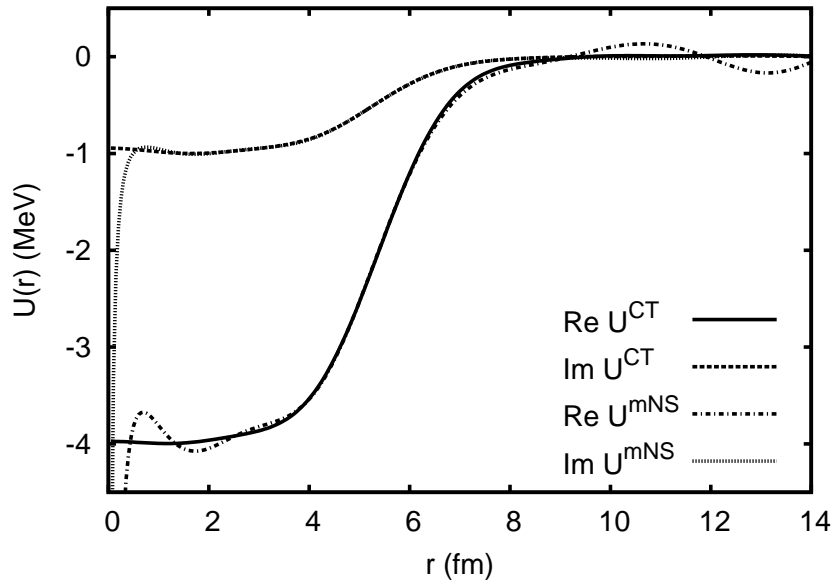
8

Fig. 2. Complex Woods-Saxon potential: Results for the inversion of 14 phase shifts at $E_{cm} = 25$ MeV using the CT- and mNS-method. The masses of the scattered particles were chosen as $M_1 = M$ and $M_2 = 20 \cdot M$, where M is the nucleon mass. Because of the good agreement of the CT inversion potential with the original Woods-Saxon-potential, the latter one is not shown in the figure.

3.2 Inversion of real n-α phase shifts derived from experiment

As an example for phase shifts related to experimental differential cross sections let us consider the elastic n-α scattering below the inelastic treshold $n + \alpha \rightarrow d + T$ at $E_n = 22.06$ MeV. An extended search for phase shifts is published by Arndt and Roper [10], the n-α scattering is reviewed by Ali et al. [11] and a theoretical summary of the inversion problem is presented by Kukulin and Mackintosh [5] where further references

can be found. Since the CT method presented in Section 2 assumes a local central potential, we have to simplify the actual problem considerably. Being aware of the spin of the neutron connected with a spin-orbit potential, of the parity-dependence of the potential, and of several theoretical treatments (see [5]) of the n-α-interaction, we restrict ourselves here to a simplified set of phase shifts obtained by Lun et al. [12] from experimental differential cross section data of [13]. Lun et al. [12] assumed the n-α-scattering as a scattering of two spin-less particles and derived the phase shifts $\delta_l^{(\mathrm{orig})}$ given in Table 1 by using Newton's iteration method.

With the CT method we calculated the potentials from the phase shifts $\delta_l^{(\mathrm{orig})}$. They are shown in Fig. 3 together with published potentials [14] re-calculated with the modified NS method and the same phase shifts. The NS method results in a nonphysical singularity near the origin whereas the CT method yields a finite potential value there. However, the potential at the origin has only a negligible effect to the re-calculated phase shifts (see Table 1) and differential elastic cross sections. We conclude that the CT and modified NS methods are nearly equivalent in the quality of inverted potentials besides the singularity of the NS method at the origin. As one can recognize in Fig. 3, the potential at the origin calculated with the CT method has an increasing deepness with energy in the investigated energy interval. This fact disagrees with microscopically and phenomenologically derived local potentials which show a decreasing deepness with energy [5,11,15]. However all the latter potentials include at least a spin-orbit potential in addition to the central potential. The shape of the obtained potentials can be nicely fitted by a Woods-Saxon form $U(r) = U_0^{\mathrm{fit}}/[1 + \exp{(r - R)/a}]$ or a Gauss form $U(r) = U_0^{\mathrm{fit}} \exp{-r^2/\sigma^2}$. The parameters of these fits are listed in Table 2.
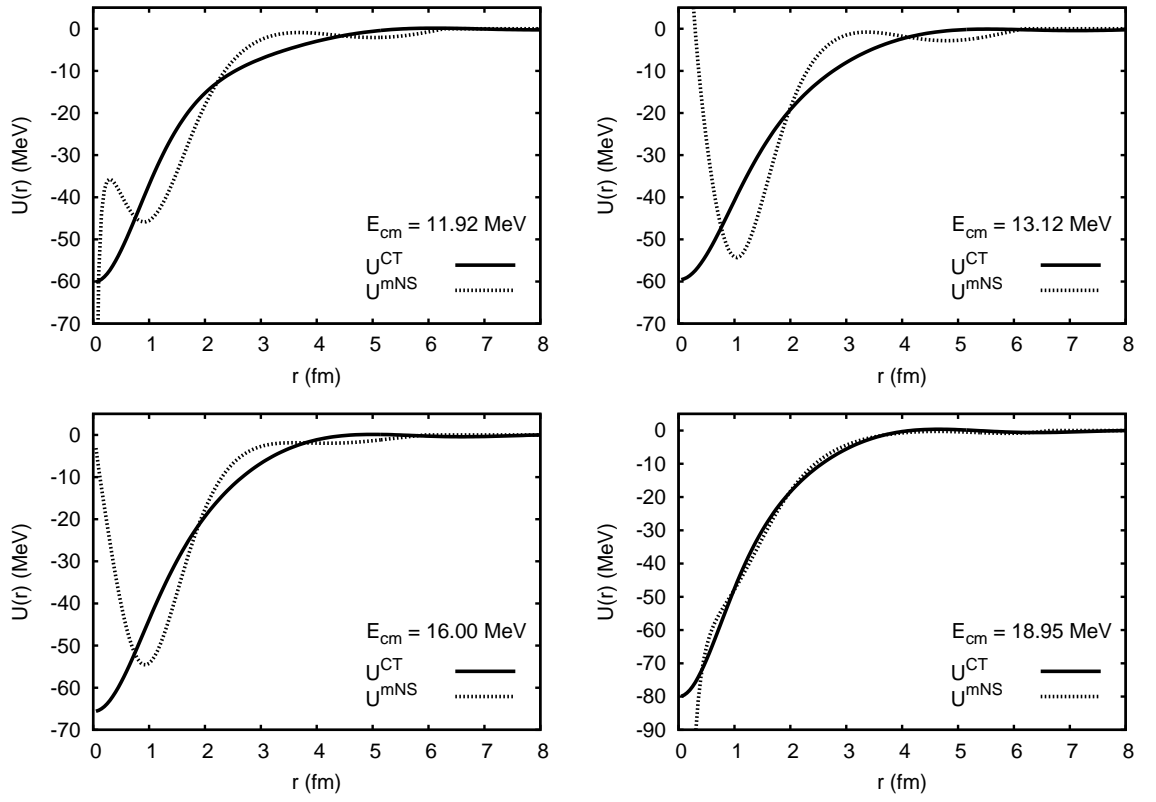
Fig. 3. Comparison of potentials inverted from real phase shifts by a CT- and mNS-calculation for n-α scattering at different energies.

Table 1: The $n - \alpha$ scattering. Entries from left to right: neutron energies in the lab and c.m. system, input angular momenta (l), calculated angular momenta (L), expansion coefficients (γ_l) [see eq. (11)], input $n - \alpha$ phase shifts ($\delta_l^{(\mathrm{orig})}$), phase shifts ($\delta_l^{(\mathrm{CT})}$) and ($\delta_l^{(\mathrm{mNS})}$) calculated with the CT and mNS inverted potentials, respectively.

E_{lab} (MeV)	$E_{\mathrm{c.m.}}$ (MeV)	l	L	γ_l	$\delta_l^{(\mathrm{orig})}$	$\delta_l^{(\mathrm{CT})}$	$\delta_l^{(\mathrm{mNS})}$
		0	-1.616	-0.302	1.824	1.809	1.823
		1	0.455	0.586	1.180	1.169	1.164
14.9	11.92	2	1.888	0.619	0.286	0.300	0.296
		3	3.002	-0.015	0.109	0.093	0.101
		4	4.019	-0.176	0.000	0.012	0.020
		0	-1.797	-0.357	1.846	1.844	1.845
		1	0.403	0.334	1.423	1.407	1.404
16.4	13.12	2	1.848	0.766	0.361	0.366	0.360
		3	3.005	-0.040	0.122	0.120	0.143
		4	4.001	-0.009	0.034	0.033	0.030
		0	-1.712	-0.346	1.742	1.745	1.739
		1	0.434	0.464	1.360	1.346	1.345
20.0	16.00	2	1.876	0.666	0.315	0.321	0.311
		3	3.019	-0.150	0.096	0.096	0.101
		4	4.008	-0.070	0.022	0.024	0.023
		0	-1.665	-0.327	1.733	1.736	1.727
		1	0.446	0.528	1.287	1.269	1.286
23.7	18.95	2	1.886	0.621	0.301	0.301	0.296
		3	3.028	-0.220	0.075	0.076	0.099
		4	3.986	0.130	0.053	0.050	0.044

Table 2: Fitted $n - \alpha$ potentials. Entries from left to right: Neutron energy $E_{\mathrm{c.m.}}$ in the c.m. system, inversion potential depth U_0^{CT}, fitted potential depth U_0^{fit}, Woods-Saxon-fit parameters R, a, Gauss-fit parameter σ and standard χ^2-test for the fitted potentials χ^2_{WS}, χ^2_{G}.

$E_{\mathrm{c.m.}}$ (MeV)	U_0^{CT} (MeV)	U_0^{fit} (MeV)	R (fm)	a (fm)	σ (fm)	χ^2_{WS}	χ^2_{G}
11.92	-60.2	-60.0	1.4	0.60	1.66	1.5	1.8
13.12	-59.6	-59.8	1.5	0.65	1.85	0.8	1.3
16.00	-65.8	-65.4	1.5	0.59	1.77	0.9	0.8
18.95	-80.0	-80.0	1.3	0.54	1.55	1.5	1.8

3.3 Inversion of the central and spin-orbit potentials from complex $n - {}^{12}\mathrm{C}$ phase shifts derived from experiment

Complex valued phase shifts describing the $n - {}^{12}\mathrm{C}$ scattering have been derived by Chen and Tornow [16] for different energies in the region $7\,\mathrm{MeV} \leq E_{\mathrm{n}}^{\mathrm{lab}} \leq 24\,\mathrm{MeV}$ using a phase shift analysis of the measured elastic cross section data. The scattering process can be described, in each partial wave l, by two phase shifts δ_l^+ and δ_l^- which contain information on both the central potential and the spin-orbit one. The central potential $U(r)$ can be determined from approximate phases given by

$$\delta_l = \frac{1}{2l+1}[(l+1)\delta_l^+ + l\delta_l^-] \ . \tag{13}$$

This expression was derived by Leeb at al. [17] and is based upon an expansion of the phase shifts where the effect of the spin-orbit potential is taken into account via a distorted wave approximation.

In order to get information on the dominating central potential we have inverted all the 88 sets of complex scattering phase shifts at different scattering energies as given by Chen and Tornow [16]. Because the potentials exhibit similar properties, only three

of them are depicted in Figure 4 and the corresponding generalized angular momenta $\{L\}$, expansion coefficients γ_l, and re-calculated phase shifts $\delta_l^{(CT)}$ and elasticities $\eta_l^{(CT)}$ are listed in Table 3. If we compare the original and re-calculated quantities, we note a larger discrepancy than in the case of inversions with real phase shifts listed in Table 1. Here, we have $|\delta_l^{(\text{orig})} - \delta_l^{(CT)}| \leq 0.11$ and $|\eta_l^{(\text{orig})} - \eta_l^{(CT)}| \leq 0.12$. Taking these deviations in mind, one should not worry about an reflection coefficient $\eta_{l=4}^{(CT)}$ ($E_n = 10.0$ MeV) slightly larger than unity.

The spin-orbit potential can be determined in the same approximation [17] as above by using the phase shifts

$$\delta_l' = \frac{1}{2l+1}[l\delta_l^+ + (l+1)\delta_l^-] \,. \tag{14}$$

These phase shifts lead to $U(r) - \frac{1}{2}V_{sl}(r)$ from which the spin-orbit potential is extracted. In Fig. 5 we present the complex spin-orbit potential for a neutron energy of $E_n = 10.0$ MeV. Here, further work will be done in order to include spin-orbit potentials directly into the Cox-Thompson method.
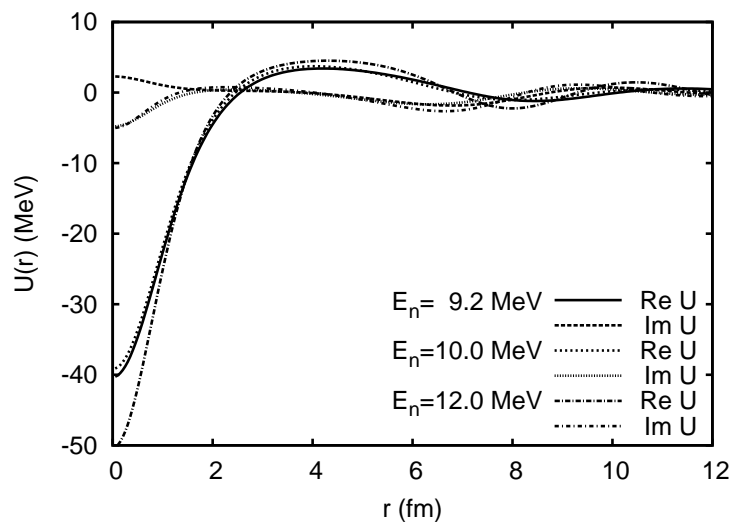

Fig. 4. Real and imaginary central potentials inverted from phase shifts of $n - {}^{12}C$ differential cross sections at the neutron energies $E_n^{\text{lab}} = 9.2, 10$ and 12 MeV.
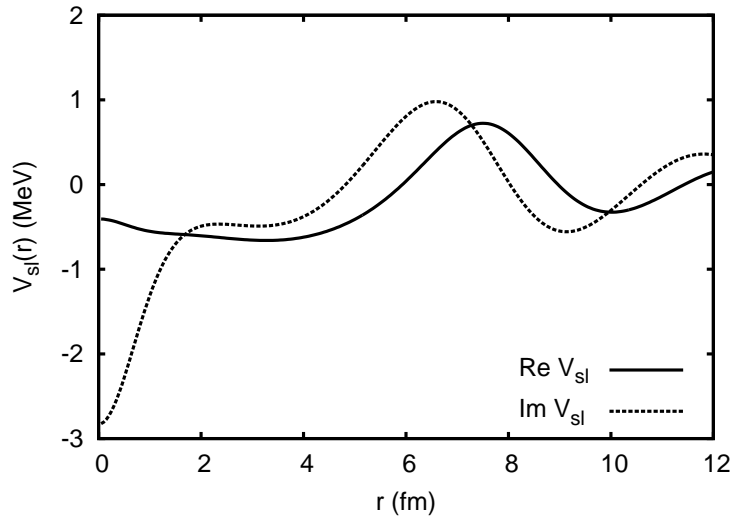
14

Fig. 5. Real and imaginary spin-orbital potentials inverted from phase shifts of $n - {}^{12}\mathrm{C}$ differential cross section at the neutron energy $E_n = 10.0$ MeV.

In general, one can see in Figure 4 that the $^{12}\mathrm{C}$ nucleus exerts a strong attractive force on the impinging nucleon. The real part of the central potential exhibits a strong minimum at zero relative distance inside the carbon nucleus. Then a characteristic maximum of about 5 MeV height follows in the region $4 \leq r \leq 5$ fm. Finally, one can observe also a shallow attraction around 8 fm.

The imaginary part of the central potential is usually weaker than the real part. It may take both negative and positive values corresponding to absorption and back-flow processes to/from the excited channels.

We remark that these model-independent features of the central potentials just derived can serve as a guide for any theoretical model study on the system $n - {}^{12}\mathrm{C}$.

Table 3: Generalized angular momenta L, expansion coefficients γ_l for the symmetric kernel and original input phase shifts $\delta_l^{(\mathrm{orig})} = \mathrm{Re}\,\delta_l$, $\eta_l^{(\mathrm{orig})} = |S_l|$ for the $n-{}^{12}\mathrm{C}$ scattering at different energies compared to $\delta_l^{(\mathrm{CT})}$ and $\eta_l^{(\mathrm{CT})}$ arising from the Cox-Thompson inversion potential.

E_{n}	l	$\mathrm{Re}(L)$	$\mathrm{Im}(L)$	$\mathrm{Re}(\gamma_l)$	$\mathrm{Im}(\gamma_l)$	$\delta_l^{(\mathrm{orig})}$	$\eta_l^{(\mathrm{orig})}$	$\delta_l^{(\mathrm{CT})}$	$\eta_l^{(\mathrm{CT})}$
	0	-0.628	-0.018	0.400	-0.112	0.857	0.700	0.848	0.670
	1	1.211	0.005	-1.086	0.340	-0.563	0.740	-0.589	0.676
9.2	2	2.409	-0.221	-1.491	1.357	-0.380	0.472	-0.320	0.523
	3	2.925	-0.122	0.209	0.610	0.098	0.744	0.049	0.670
	4	4.010	-0.072	-0.192	0.546	0.010	0.971	0.067	0.995
	0	-0.581	-0.085	0.433	-0.117	0.827	0.580	0.811	0.582
	1	1.226	0.001	-1.165	0.320	-0.562	0.723	-0.580	0.686
10.0	2	2.349	-0.192	-1.407	1.111	-0.365	0.526	-0.326	0.579
	3	2.981	-0.073	0.027	0.361	0.057	0.846	0.028	0.775
	4	4.010	-0.062	-0.142	0.463	0.021	0.959	0.058	1.015
	0	-0.615	-0.068	0.452	-0.136	0.522	0.580	0.548	0.607
	1	1.152	0.011	-0.981	0.213	-0.737	1.0	-0.779	0.882
12.0	2	2.905	-0.338	-2.882	1.395	-0.689	0.560	-0.583	0.570
	3	2.613	0.037	0.611	0.955	0.172	0.643	0.087	0.598
	4	4.099	-0.146	-0.980	0.932	0.021	0.831	0.113	0.826

4. Summary and conclusions

We have generalized the Cox-Thompson inverse scattering method at fixed energy to derive complex inverse potentials from phase shifts. Corresponding basic formulas, Eqs. (7) and (10), have been presented relating input phase shifts and shifted angular momentum quantum numbers from which the inverse potentials can been calculated via Eqs. (2) and (6).

The first application of the CT method to experimental $n - \alpha$ phase shifts resulted in inversion potentials which can be fitted by Woods-Saxon and Gauss forms within the energy range considered. For the complex $n-^{12}\text{C}$ data we have derived model-independent complex central and spin orbital potentials.
Interesting phase shift data of rich complexity are derived for heavy-ion scattering. Therefore, we can conclude from the results obtained above for the n-nucleus scattering that the CT inverse method deserves to be extended further to be able to treat phase shift data originated from charged particle collisions, too.

Appendix

The first term in the parenthesis of the rhs of Eq. (1) can be written as

$$K'(r,r) = \sum_L (A'_L(r)u_L(r) + A_L(r)u'_L(r)). \qquad (A1)$$

17

After solution for the set T of one of the basic equations (7) or (10), the coefficient functions can be determined from Eq. (6) as

$$A_L(r) = \sum_{l \in S} \left(\tilde{W}^{-1}\right)_{Ll}(r)v_l(r) \qquad (A2)$$

with the inverse of the square matrix

$$\tilde{W}_{lL}(r) = W[u_L, v_l]/[l(l+1) - L(L+1)] \qquad (A3)$$

where W is the Wronskian of the independent solutions $u_{L \in T}$ and $v_{l \in S}$.

Differentiating Eq. (6) yields the second unknown quantity of interest in Eq. (A1), namely $A'_L(r)$, which can be calculated from the Wronskian and the pre-determined A_L's as:

$$A'_L(r) = \sum_{l \in S} \left(\tilde{W}^{-1}\right)_{Ll}(r) \left(v'_l(r) - \sum_{L' \in T} \tilde{W}'_{lL'}(r)A_{L'}(r) \right) \qquad (A4)$$

with

$$\tilde{W}'_{lL}(r) = u_L(r)v_l(r)/r^2. \qquad (A5)$$

Then, the inverse potential can easily be calculated by using Eqs. (1), (2), and (A1).

We have also to evaluate the regular Riccati-Bessel function

$$u_L(r) = \sqrt{\frac{r\pi}{2}}J_{L+\frac{1}{2}}(r) \qquad (A6)$$

with complex indices L. This we can accomplish by using the ascending series representation

$$J_\nu(r) = \left(\frac{r}{2}\right)^\nu \sum_{k=0}^\infty \frac{\left(-\frac{r^2}{4}\right)^k}{k!\Gamma(\nu+k+1)} \qquad (A7)$$

for the Bessel-J function of complex order ν. All we need is thus to calculate the gamma function for complex argument which can easily be accomplished using the Euler formula which represents it as an infinite product of rapid convergence.

18

Acknowledgments

References

[1] I.M. Gel'fand and B.M. Levitan 1951 *Dokl. Akad. Nauk. USSR* **77** 557, translated in 1955 *Am. Math. Soc. Transl. Ser.* **2** 1, 253; V.A. Marchenko 1955 *Dokl. Akad. Nauk. USSR* **104** 695, translated in 1956 *Math. Rev.* **17** 740

[2] I. Lipperheide, L. Fiedeldey 1978 *Z. Phys.* **286** 45; *ibid* 1981 **301** 81

[3] R. G. Newton 1962 *J. Math. Phys.* **3** 75; P. C. Sabatier 1966 *J. Math. Phys.* **7** 1515

[4] M. Münchow and W. Scheid 1980 *Phys. Rev. Lett.* **44** 1299

[5] V. I. Kukulin and R. S. Mackintosh 2004 *J. Phys. G: Nucl. Part. Phys.* **30** R1

[6] J. R. Cox and K. W. Thompson 1970 *J. Math. Phys.* **11** 805; *ibid* 1970 **11** 815

[7] B. Apagyi, Z. Harman and W. Scheid 2003 *J. Phys.* A **36** 4815

[8] R. G. Airapetyan, A. G. Ramm and A. B. Smirnova 1999 *Phys. Lett.* A **254** 141

[9] A. G. Ramm and S. Gutman 2001 *Applicable Analysis* **78** 207

[10] R. A. Arndt and L. D. Roper 1970 *Phys. Rev.* C **1** 903

[11] S. Ali, A. A. Z. Ahmad and N. Ferdous 1985 *Rev. Mod. Phys.* **57** 923

[12] D.R. Lun, L.J. Allen and K. Amos 1994 *Phys. Rev.* A **50** 4000

[13] R. Malaroda, G. Poiani and G. Pisent 1963 *Phys. Lett.* **5** 205; R. E. Shamu and J. G. Jenkin 1964 *Phys. Rev.* **135** B99

[14] N. Alexander, K. Amos, B. Apagyi and D. R. Lun 1996 *Phys. Rev.* C **53** 88

[15] N. Vinh Mau in *Microscopic Optical Potentials* (H. V. von Geramb ed, Lecture Notes in Physics, Vol. 89, Springer, 1979) p. 40; M. Lassaut and N. Vinh Mau 1977 *Phys. Lett.* B **70** 14 and 1980 *Nucl. Phys.* A **349** 372

[16] Z. P. Chen and W. Tornow 2005 *J. Phys. G: Nucl. Part. Phys.* **31** 1249

[17] H. Leeb, H. Huber and H. Fiedeldey 1995 *Phys. Lett.* B **344** 18